Physica A 511 (2018) 272–279

Contents lists available at ScienceDirect

Physica A

journal homepage: www.elsevier.com/locate/physa

A general social contagion dynamic in interconnected lattices

Panpan Shu [a], Wei Wang [b,*], H. Eugene Stanley [c], Lidia A. Braunstein [d,c]

[a] Xi'an University of Technology, Xi'an 710054, China
[b] Cybersecurity Research Institute, Sichuan University, Chengdu 610065, China
[c] Center for Polymer Studies and Department of Physics, Boston University, Boston, MA 02215, USA
[d] Instituto de Investigaciones Físicas de Mar del Plata (IFIMAR), Departamento de Física, Facultad de Ciencias Exactas y Naturales, Universidad Nacional de Mar del Plata, CONICET, Funes 3350, (7600) Mar del Plata, Argentina

HIGHLIGHTS

- We propose a generalized social contagion model on two interconnected planar lattices.
- The dependency of prevalence on the transmission rate is always continuous.
- The social contagions could be strongly promoted.

ARTICLE INFO

Article history:
Received 8 May 2018
Received in revised form 2 July 2018
Available online 26 July 2018

Keywords:
Complex networks
Spreading dynamics
Social contagions

ABSTRACT

Research on dynamical processes in interconnected spatial networks has expanded in recent years, but there has been little focus on social contagions. Using a general social contagion model, we numerically study how an interconnected spatial system composed of two interconnected planar lattices influences social contagion dynamics. When information is transmitted and allows for a probability of behavior adoption, strongly interconnected lattices stimulate the contagion process and significantly increase the final density of adopted individuals. We perform a finite-size analysis and confirm that the dependency of prevalence on the transmission rate is continuous regardless of the adoption probability. The prevalence grows discontinuously with the adoption probability even when the transmission rate is low. Although a high transmission rate or a high adoption probability increases the final adopted density in weak interconnected lattices, the prevalence always grows continuously in these networks. These findings help us understand social contagion dynamics in interconnected lattices.

1. Introduction

Many real-world networks are systems in which isolated networks are interconnected [1–3]. Nodes in communications networks, for example, are strongly interconnected with nodes in electrical power networks [2]. These systems have both internal connectivity links within each individual network and also interconnections between the networks that significantly influence the dynamical processes that spread through them [4–8]. In epidemic propagation a susceptible individual in contact with an infected individual becomes infected with a probability β. For example in the susceptible–infected–susceptible (SIS) epidemic model, above a critical threshold β_c the epidemic is not able to propagate in a single network, but a global endemic state may occur even in a coupled system with a small number of interlink connections [9]. In strongly interconnected network systems, the susceptible–infected–recovered (SIR) epidemic model does not spread below a critical

* Corresponding author.
E-mail address: wwzqbx@hotmail.com (W. Wang).

https://doi.org/10.1016/j.physa.2018.07.049
0378-4371/

infection strength, but in weakly coupled network systems a mixed phase transition of the final epidemic size occurs below this critical value [10]. Many real-world systems such as power grids and communication networks are spatially embedded [11–14] and are typically modeled using Euclidean lattices [15,16]. The heterogeneous coupling between interconnected lattices strongly promotes cooperation in the prisoner's dilemma game [17]. In the SIS model, when infection rates are low the interconnected spatial constraints in a lattice causes the fraction of infected individuals in interconnected lattices to be lower than in interconnected Erdős–Rényi (ER) networks that are characterized by a Poisson degree distribution with an average degree $\langle k\rangle = 4$ [18]. When infection rates are high, however, the infection density is higher in interconnected lattices than in interconnected ER networks [18].

Unlike the dynamics of epidemics, the dynamics of social contagions [19–25], which can range from the adoption of social innovations [26–30] to the spread of healthy behaviors in response to patterns of human obesity [31], are strongly affected by social reinforcement. Previous studies have shown that multiple affirmations of the credibility of a piece of news or a new trend strongly affect social contagion. To be specific, the probability that an individual will adopt a new social behavior depends on social reinforcement, which is often measured in terms of the number of contacts an individual has with credible neighbors who have already adopted the behavior [32–36]. In a threshold model widely used to describe the social reinforcement effect, each individual is either susceptible (S) or adopted (A) [37]. A susceptible individual adopts a social behavior when the number or fraction of adopted neighbors exceeds an adoption threshold. In the numerous studies that show how network structure strongly influences this threshold model [38–43], the social reinforcement of social contagions is powered by nonredundant information transmissions from neighbors, i.e., the repeat transmission of the same information between two neighbors is disallowed. Because in some examples of social contagion, such as the spread of high-risk social movements, avant garde fashions, and unproven technologies [35], information transmissions between two individuals is only partially effective because susceptible individuals regard the credibility and legitimacy of the new behavior to be limited [31]. Based on the nonredundant social contagion dynamic in an isolated complex network, Wang et al. [20] found a phase transition in which the dependence of the final adoption size on the transmission probability changes from discontinuous to continuous [20]. However spatial characteristics of complex networks are often neglected in the study of nonredundant social contagions dynamics.

Here we use a novel social contagion model to study non-redundant social contagions in interconnected spatial networks. We show how the interconnected lattices influence the level of social contagion, and we explore the role of interconnections in phase transitions. In general, we find the discontinuous phase transition in the order parameter of the giant connected cluster of adoption prevalence in strongly interconnected lattice networks and the continuous phase transition in weakly interconnected lattice networks. Specially, although the social contagions could be strongly promoted high adoption probability in both weak and strong interconnected networks, the type of phase transition is continuous. The finite-size analyses are performed to locate the scaling relations near the transition points of discontinuous and continuous phase transitions.

We organize the paper as follows. In Section 2 we describe an interconnected spatial network and a social dynamics model. In Section 3 we use a finite-size analysis to study the phase transition. In Section 4 we present our conclusions.

2. Model

2.1. Interconnected lattice network

Many real-world systems, such as power grids and communication networks, are spatially embedded and are typically modeled using Euclidean lattices [15,16]. Because interconnections between networks can significantly influence the dynamic processes that spread through them, our interconnected spatial network is composed of two identical square lattices A and B of linear size L and $N = L \times L$ nodes with periodic boundaries. The two lattices represent two different social groups. For example, a couple can discuss household products in their friendship group. A wife or husband adopts a new product if many of their friends have adopted it. It either the wife or husband adopts it, the other also adopts it. In each lattice all nodes are arranged in a matrix of $L \times L$, and each node is connected to its four lattice neighbors via connectivity links (i.e., links between two nodes in the same lattice). Because there may be interconnections between individuals in group A with individuals in group B (e.g., relationships between friends), we randomly select a fraction p of nodes in lattice A to be connected with a random fraction p of nodes in lattice B. Here each interconnected node has only one interconnected link. The total number of interconnected links in the interconnected spatial network is determined by the parameter p, i.e., the number of interconnected links is pN. Note that the greater the number of interconnected links the higher the level of interconnection between the two lattices. For simplicity we define the networks with a large value of p to be strongly interconnected, and those with a small value of p to be weakly interconnected.

2.2. Dynamic of social contagions

We designate each node in the interconnected lattices to be either susceptible (S), adopted (A), or recovered (R). Susceptible individuals have not adopted the behavior and are susceptible to receiving behavior information. Adopted individuals have adopted the behavior and are able to transmit the information to susceptible neighbors. Recovered individuals have become immune to the behavior and are no longer a part of the system. Within the same lattice, individuals

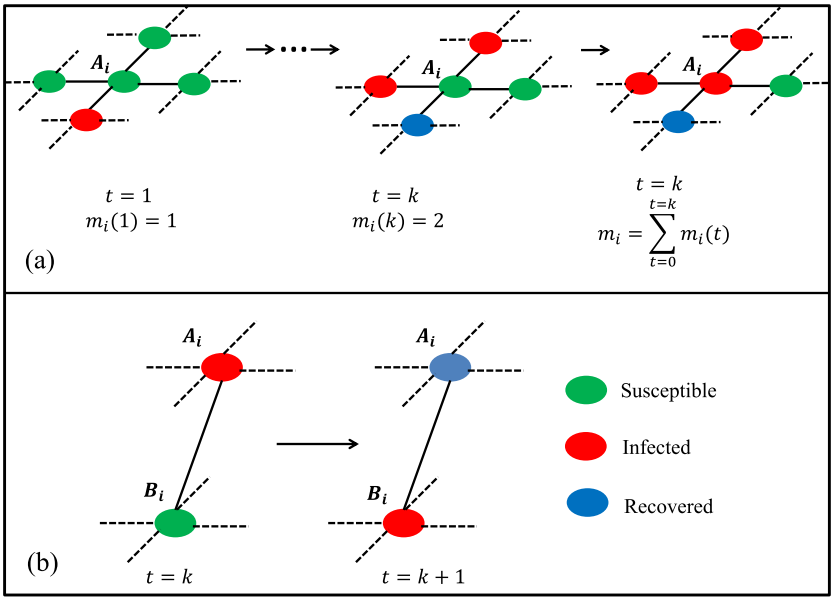

Fig. 1. (Color online) Sketch of the ways of adopting the social behavior on interconnected lattices. (a) Intralayer propagation: At $t = 1$, the individual A_i is successfully exposed to one adopted neighbor, and now the number of new received information is $m_i(1) = 1$ and m_i increases by 1. There are no more new adopted neighbors over the next $k - 2$ time steps, and m_i remains unchanged. At $t = k$, two new adopted neighbors successfully transmit the information to i, and now $m_i(k) = 2$. The individual A_i becomes adopted with probability $\pi(m_i)$, where $m_i = \sum_{t=0}^{t=k} m_i(t) = 3$. (b) Interlayer propagation: At $t = k$, A_i is adopted. At $t = k + 1$, its interconnected node B_i becomes adopted due to the interlayer propagation.

can retain their memory of previous behavior information received from neighbors. A susceptible individual adopts the new behavior with a probability that depends on the cumulative units of information received from adopted neighbors and become adopted. We designate this type of adoption *intralayer propagation*. Taking into account the nonredundant information diffusion in the social contagion processes [35], a susceptible individual i is assumed to adopt the behavior with a probability

$$\pi(m_i) = 1 - (1 - \epsilon)^{m_i}, \tag{1}$$

where m_i is the cumulative number of information units a susceptible individual has received from neighbors in the single lattice. For example, a susceptible node A_i becomes adopted with probability $\pi(m_i)$ at time $t = k$, where $m_i = \sum_{t=1}^{t=k} m_i(t)$, $m_i(t)$ is the number of information units A_i receives from its adopted neighbors at time t [see Fig. 1(a)], and ϵ is the unit adoption probability. A susceptible individual adopts the new behavior after its corresponding interconnected node in the other lattice has adopted it. We designate this type of adoption *interlayer propagation* [see Fig. 1(b)].

We implement the social contagion dynamic simulation as follows. At the initial stage we randomly select a density of 0.05% of lattice A individuals in the system to be adopted, and we designate all others susceptible. These adopted seeds produce several isolated connected clusters of adopted nodes. Each susceptible individual receives m_i information units from adopted neighbors, $m_i = 0$ initially. At each time step, each adopted individual transmits with a probability β the behavior information to susceptible neighbors in the same lattice via connectivity links. When a susceptible node i receives the information from an adopted neighbor for the first time, m_i increases by one and the adoption probability becomes $\pi(m_i + 1)$ and π increases with m_i and ϵ. The information transmission from the adopted neighbor to node i is forbidden in the following contagion process, which means that the information from an adopted node to one of its susceptible neighbors can only be transmitted once. When node i becomes adopted, interlayer infection causes the susceptible interconnected node to become adopted at the next time step. Infected nodes can then lose interest in the social behavior and with a probability μ become recovered. When an adopted node recovers it no longer propagates the social behavior. Each time step is discrete and increases by $\Delta t = 1$. The dynamics of social contagion evolve until the system reaches the steady state where there are no more adopted nodes in the network, and the only possible states are S or R. Thus in the steady state the fraction of nodes in the giant component of recovered nodes is the order parameter of the phase transition.

3. Results

We here perform extensive numerical simulations of social contagions in interconnected lattice networks. We define the effective infection rate $\lambda = \beta/\mu$, and set the recovery probability μ to 1. Fig. 2 shows an analysis of the prevalence (i.e., the average density of final recovered individuals) as a function of the transmission probability λ in lattice A. Here the

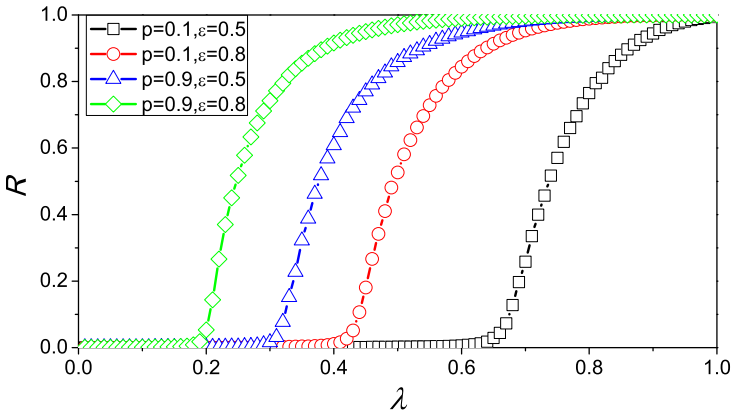

Fig. 2. (Color online) The prevalence R as a function of λ within different values of p and ϵ. We perform the experiments on 10^2 different networks with $N = 10^4$, each of which are tested in 10^3 independent realizations.

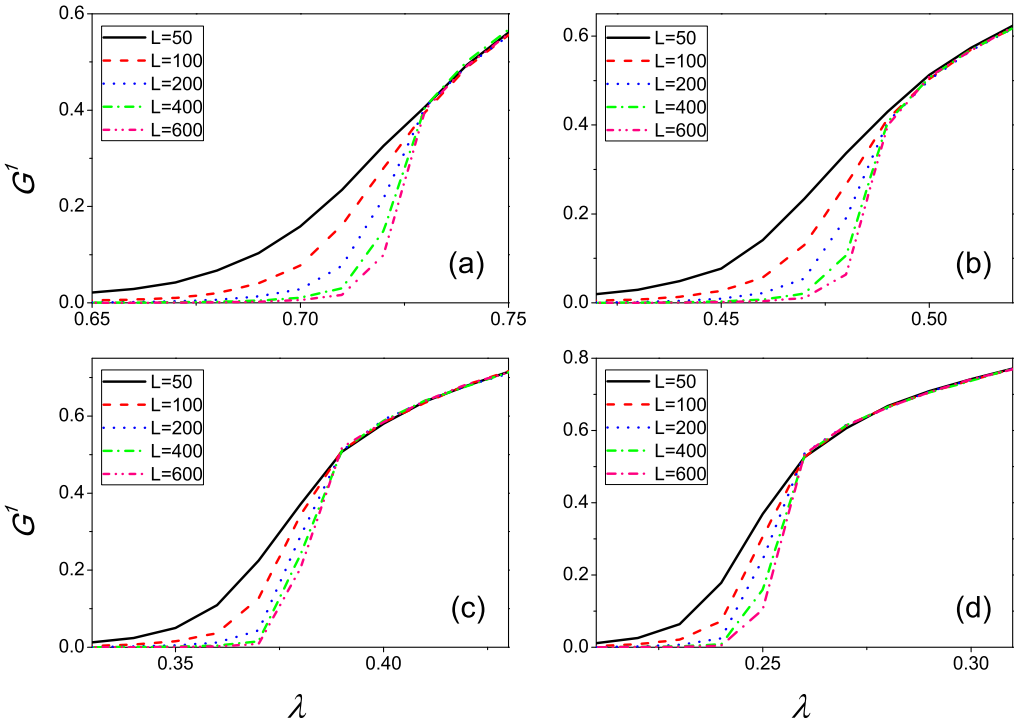

Fig. 3. (Color online) The fraction of nodes in the giant component of the recovered nodes G^1 as a function of λ within different L. In subfigures (a)–(d), the parameters are respectively chosen as $p = 0.1, \epsilon = 0.5$, $p = 0.1, \epsilon = 0.8$, $p = 0.9, \epsilon = 0.5$ and $p = 0.9, \epsilon = 0.8$. We perform the experiments on 10^2 different networks, each of which are tested in 10^3 independent realizations.

large adoption probability (i.e., $\epsilon = 0.8$) ensures a high information adoption rate and increases the prevalence. Networks with high p values have a high level of interlayer infection and propagate the behavior more easily than when the p value is low. Fig. 2 shows that there is a phase transition in the prevalence R at a critical threshold λ_c that depends on the fraction of interconnected nodes p and the adoption probability ϵ. As p and ϵ increase, the critical threshold λ_c decreases, and the system becomes more resilient to be in the adopted state. Because networks A and B are symmetrical, we show only R in network A.

Fig. 3 uses a finite-size analysis to study the order parameter of the phase transitions (i.e., the fraction of nodes in the giant component of recovered nodes G^1) for different lattice sizes L. In each subgraph the difference in the values of G^1 for different L is very small when λ is larger than some value. For example, the values of G^1 for different L are approximately

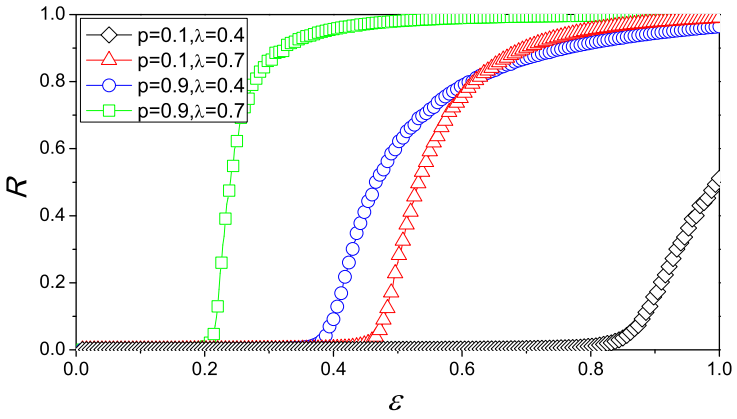

Fig. 4. (Color online) The prevalence R as a function of ϵ within different values of p and λ. We perform the experiments on 10^2 different networks with $N = 10^4$, each of which are tested in 10^3 independent realizations.

the same when $\lambda > 0.73$ for $p = 0.1, \epsilon = 0.5$. Note that although parameters p and ϵ strongly affect the dependency of prevalence on the transmission rate λ, there is always a continuous phase transition [44].

For a given p and a transmission probability λ above the critical threshold λ_c, we plot the prevalence as a function of ϵ [see Fig. 4]. When λ and p are small, both the intralayer propagation and the interlayer propagation are suppressed. Although the adoption probability is large, the social contagion cannot spread. The information transmission among neighbors within the same lattice increases for large value of λ, and this further stimulates the adoption of the social behavior, especially when p is large. Fig. 4 shows that there is a phase transition in the prevalence R at a critical threshold ϵ_c that depends on the fraction of interconnected nodes p and the transmission probability λ. As p and λ increase, the critical threshold ϵ_c decreases, and the adopted state of the system becomes more resilient.

Fig. 5 shows the order parameter of the phase transition G^1 for different lattice sizes L. Note that the values of G^1 for different L values are approximately the same when λ is larger than some value for $p = 0.1$, $\lambda = 0.4$, and $\lambda = 0.7$, but that the curves intersect at $\epsilon \approx 0.476$ for $p = 0.9$, and $\lambda = 0.4$ and $\epsilon \approx 0.228$ for $p = 0.9$, and $\lambda = 0.7$. This indicates that parameter p strongly affects both prevalence versus ϵ and the type of phase transition. When p is large, a small fraction of initial spreaders can stimulate the discontinuous dependency of G^1 on ϵ. When p is small, the social behavior spreads as a continuous phase transition [44].

To locate the critical point of the transition (i.e., λ_c for fixed p and ϵ or ϵ_c for fixed p and λ) [45,46], in the discontinuous phase transition we calculate the number of iterations (NOI) during which at least one new individual adopts the behavior [20], and in the continuous phase transition we calculate the fraction of nodes in the second-largest components of the recovered nodes G^2. The NOI exhibit a maximum value at the critical point of discontinuous phase transition, and the G^2 exhibits a maximum value at the critical point of continuous phase transition. Because Fig. 5 shows the continuous phase transition for $p = 0.1$, $\lambda = 0.4$ and the discontinuous phase transition for $p = 0.9$, $\lambda = 0.7$, we show the analysis of the critical point using only these parameters in the example in Fig. 6.

Fig. 6(a) shows that when $p = 0.1$, $\lambda = 0.4$, and the peak of G^2 versus ϵ shifts to the right as L increases. The value of ϵ that corresponds to the peak for each L is defined to be the critical point of the continuous phase transition (i.e., $\epsilon_c^{II}(L)$). To find the scaling relation near the critical points [47], we use the least-squares method to fit $\epsilon_c^{II} - \epsilon_c^{II}(L)$ versus $1/L$ [see Fig. 6(b)], and find that $\epsilon_c^{II} - \epsilon_c^{II}(L) \sim (1/L)^{0.5516}$ at $\epsilon_c^{II} = 0.9875$. Fig. 6(c) shows that when $p = 0.9$, $\lambda = 0.7$, and the peak of the NOI versus ϵ shifts to the left with L. We define the value of ϵ corresponding to the peak for each L to be the critical point of the discontinuous phase transition (i.e., $\epsilon_c^I(L)$). We then use the least-squares method to fit $\epsilon_c^I(L) - \epsilon_c^I$ versus $1/L$ [see Fig. 6(d)], and find that $\epsilon_c^I(L) - \epsilon_c^I \sim (1/L)^{0.2232}$ at $\epsilon_c^I = 0.2089$.

4. Conclusions

We have studied social contagions in interconnected lattices and propose a general threshold model to describe the social reinforcement of social contagions. Our model shows that a susceptible individual adopts a new behavior with a probability proportional to the number of cumulative units of information they have received from adopted neighbors in the same lattice. They also adopt a new behavior if their interconnected node in the other lattice has adopted it. We first investigate the prevalence versus the transmission rate λ. Although a high adoption probability ϵ strongly promotes social contagions in both weakly and strongly interconnected networks, the phase transition of the prevalence is continuous. For a given transmission rate, we study prevalence versus adoption probability ϵ and find that a strongly interconnected structure increases the prevalence. In strongly interconnected networks we find discontinuous phase transitions even when the transmission rate is low. In weakly interconnected networks we find continuous phase transitions. We use a finite-size

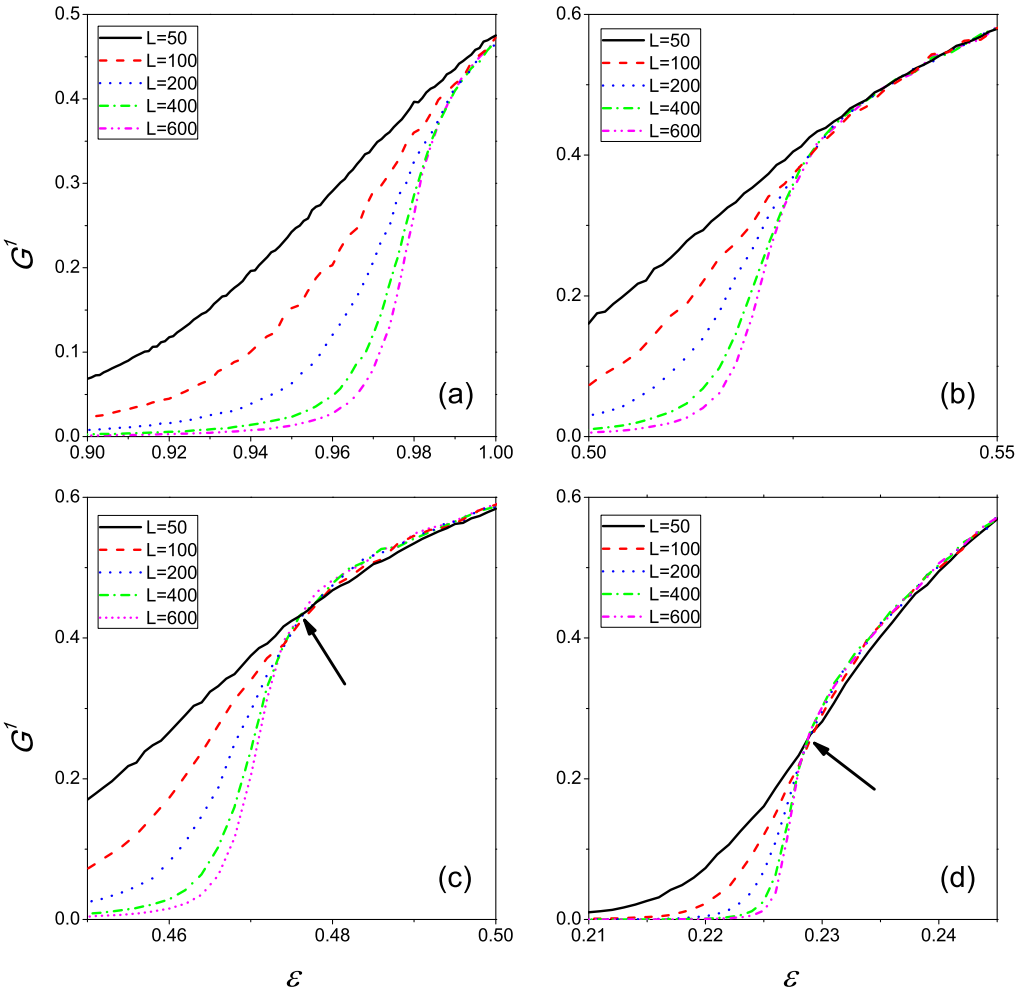

Fig. 5. (Color online) The fraction of nodes in the giant component of the recovered nodes G^1 as a function of ϵ within different L. In subfigures (a)–(d), the parameters are respectively chosen as $p = 0.1$, $\lambda = 0.4$, $p = 0.1$, $\lambda = 0.7$, $p = 0.9$, $\lambda = 0.4$ and $p = 0.9$, $\lambda = 0.7$. The results are averaged over $10^2 \times 10^3$ independent realizations in 10^2 networks.

analysis to locate scaling relations near the transition points both in discontinuous and continuous phase transitions. For example, when $p = 0.1$, $\lambda = 0.4$, the scaling relation is $\epsilon_c^{II} - \epsilon_c^{II}(L) \sim (1/L)^{0.5516}$ at $\epsilon_c^{II} = 0.9875$. When $p = 0.9$, $\lambda = 0.7$, we find that $\epsilon_c^{I}(L) - \epsilon_c^{I} \sim (1/L)^{0.2232}$ at $\epsilon_c^{I} = 0.2089$. Our results indicate that spatial interconnections are important in complex contagions, and they may help us understand the phase transitions that occur in the social contagion process.

Our theoretical research here on the dynamics of social contagions could have a reference value when predicting and understanding the spread of news, products, and political points of view, but further theoretical studies are needed because the non-Markovian character of our model and the non-local tree-like structure of our interconnected lattice make describing the dynamical correlations among the states of neighbors difficult. The social contagions dynamics in interconnected lattices with arbitrary interconnections for each node deserve further study. In addition, the integrative effect of social contagion dynamics on the phase transition when there is limited contact ability [21], co-infections [48], a multilayer system [3], or temporal interactions [49] should be further explored.

Acknowledgments

This work was supported by National Natural Science Foundation of China (Grant No. 61703330), and China Postdoctoral Science Foundation, China (Grant No. 2018M631073). The Boston University Center for Polymer Studies, USA is supported by NSF, USA Grants PHY-1505000, CMMI-1125290, and CHE-1213217, and by DTRA, USA Grant HDTRA1-14-1-0017. LAB thanks UNMdP and CONICET (PIP 00443/2014) for financial support

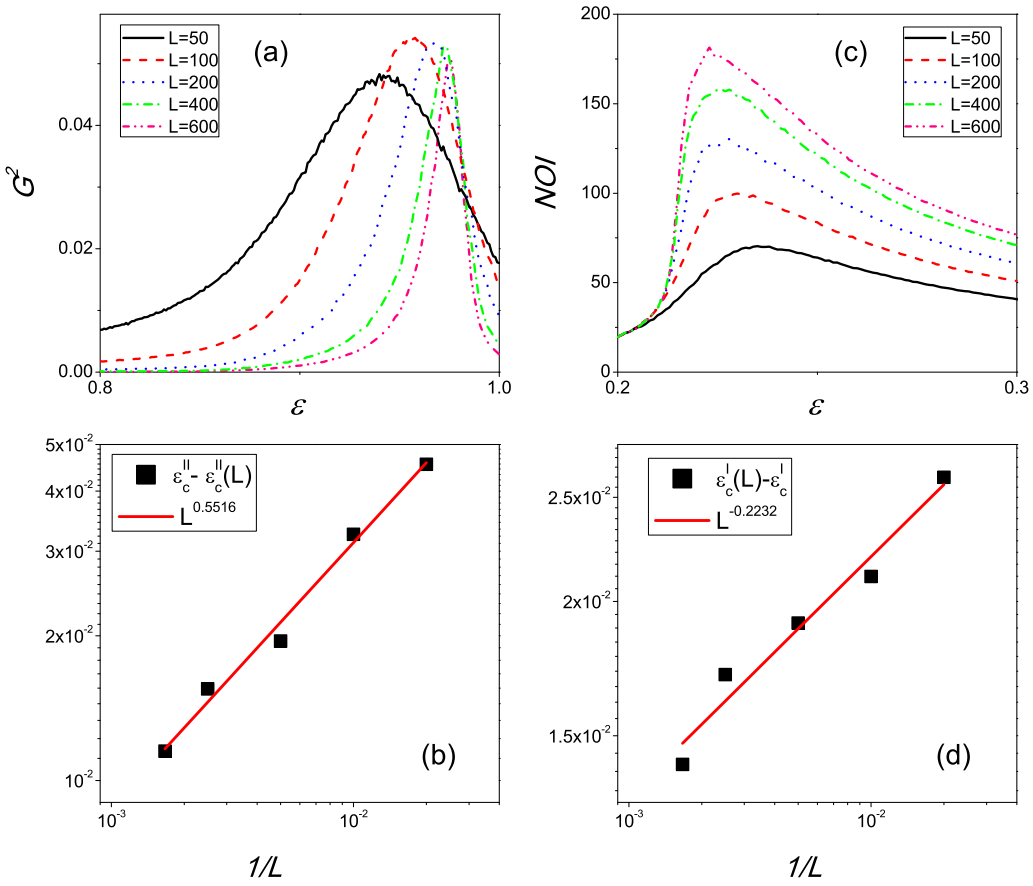

Fig. 6. (Color online) The finite-size analyses near the critical points for $p = 0.1$, $\lambda = 0.4$ (a–b) and $p = 0.9$, $\lambda = 0.7$ (c–d). (a) G^2 versus ϵ. (b) $\epsilon_c^{II} - \epsilon_c^{II}(L)$ versus $1/L$. (c) *NOI* versus ϵ. (d) $\epsilon_c^{I}(L) - \epsilon_c^{I}$ versus $1/L$. The arrows in (c) and (d) mark the intersection points. The results are averaged over $10^2 \times 10^3$ independent realizations in 10^2 networks.

References

[1] M. Barthélemy, Spatial networks, Phys. Rep. 499 (2011) 1–101.
[2] D. Li, K. Kosmidis, A. Bunde, S. Havlin, Dimension of spatially embedded networks, Nat. Phys. 7 (2011) 481–484.
[3] S. Boccaletti, G. Bianconi, R. Criado, C.I. del Genio, J. Gómez-Gardeñes, M. Romance, I. Sendiña Nadal, Z. Wang, M. Zanin, The structure and dynamics of multilayer networks, Phys. Rep. 544 (2014) 1–122.
[4] S.-W. Son, P. Grassberger, M. Paczuski, Percolation transitions are not always sharpened by making networks interdependent, Phys. Rev. Lett. 107 (2011) 195702.
[5] H. Wang, Q. Li, G. D'Agostino, S. Havlin, H.E. Stanley, P.V. Mieghem, Effect of the interconnected network structure on the epidemic threshold, Phys. Rev. E 88 (2013) 022801.
[6] L.M. Shekhtman, Y. Berezin, M.M. Danziger, S. Havlin, Robustness of a network formed of spatially embedded networks, Phys. Rev. E 90 (2014) 012809.
[7] B. Wang, G. Tanaka, H. Suzuki, K. Aihara, Epidemic spread on interconnected metapopulation networks, Phys. Rev. E 90 (2014) 032806.
[8] R.G. Morris, M. Barthelemy, Transport on coupled spatial networks, Phys. Rev. Lett. 109 (2012) 128703.
[9] A. Saumell-Mendiola, M.Á. Serrano, M. Boguñá, Epidemic spreading on interconnected networks, Phys. Rev. E 86 (2012) 026106.
[10] M. Dickison, S. Havlin, H.E. Stanley, Epidemics on interconnected networks, Phys. Rev. E 85 (2012) 066109.
[11] L. Wang, J.T. Wu, Characterizing the dynamics underlying global spread of epidemics, Nature Commun. 9 (2018) 218.
[12] J.-B. Wang, L. Wang, X. Li, Identifying spatial invasion of pandemics on metapopulation networks via anatomizing arrival history, IEEE Trans. Cybern. 46 (2016) 2782–2795.
[13] D. He, R. Lui, L. Wang, C.K. Tse, L. Yang, L. Stone, Global spatio-temporal patterns of influenza in the post-pandemic era, Sci. Rep. 5 (2015).
[14] L. Wang, X. Li, Spatial epidemiology of networked metapopulation: an overview, Chin. Sci. Bull. 59 (2014) 3511–3522.
[15] J.M. Kleinberg, Navigation in a small world, Nature 406 (2000) 845–845.
[16] J. Gao, T. Zhou, Y. Hu, Bootstrap percolation on spatial networks, Sci. Rep. 5 (2015) 14662.
[17] C.-Y. Xia, X.-K. Meng, Z. Wang, Heterogeneous coupling between interdependent lattices promotes the cooperation in the Prisoner's Dilemma game, PLoS One 10 (2015) e0129542.
[18] D. Li, P. Qin, H. Wang, C. Liu, Y. Jiang, Epidemics on interconnected lattices, Europhys. Lett. 105 (2014) 68004.
[19] R.M. Bond, C.J. Fariss, J.J. Jones, A.D.I. Kramer, C. Marlow, J.E. Settle, J.H. Fowler, A 61-million-person experiment in social influence and political mobilization, Nature 489 (2012) 295–298.
[20] W. Wang, M. Tang, H.-F. Zhang, Y.-C. Lai, Dynamics of social contagions with memory of non-redundant information, Phys. Rev. E 92 (2015) 012820.
[21] W. Wang, P. Shu, Y.-X. Zhu, M. Tang, Y.-C. Zhang, Dynamics of social contagions with limited contact capacity, Chaos 25 (2015) 103102.

[22] W. Wang, M. Tang, P. Shu, Z. Wang, Dynamics of social contagions with heterogeneous adoption thresholds: crossover phenomena in phase transition, New J. Phys. 18 (2016) 013029.
[23] Z. Ruan, G. Iñiguez, M. Karsai, J. Kertész, Kinetics of social contagion, Phys. Rev. Lett. 115 (2015) 218702.
[24] E. Cozzo, R.A. Baños, S. Meloni, Y. Moreno, Contact-based social contagion in multiplex networks, Phys. Rev. E 88 (2013) 050801(R).
[25] T. Wu, X. Chen, Y. Guo, Full-scale cascade dynamics prediction with a local-first approach, Knowl.-Based Syst. 465 (2016) 662–672.
[26] A. Czaplicka, R. Toral, M. San Miguel, Competition of simple and complex adoption on interdependent networks, Phys. Rev. E 94 (2016) 062301.
[27] F.V. Rojas, F. Vazquez, Interacting opinion and disease dynamics in multiplex networks: discontinuous phase transition and non-monotonic consensus times, Phys. Rev. E 95 (2017) 052315.
[28] Y. Hu, S. Havlin, H.A. Makse, Conditions for viral influence spreading through multiplex correlated social networks, Phys. Rev. X 4 (2014) 021031.
[29] L.K. Gallos, D. Rybski, F. Liljeros, S. Havlin, H.A. Makse, How people interact in evolving online affiliation networks, Phys. Rev. X 2 (2012) 031014.
[30] H.P. Young, The dynamics of social innovation, Proc. Natl. Acad. Sci. USA 108 (2011) 21285–21291.
[31] D. Centola, An experimental study of homophily in the adoption of health behavior, Science 334 (2011) 1269–1272.
[32] P.S. Dodds, D.J. Watts, Universal behavior in a generalized model of contagion, Phys. Rev. Lett. 92 (2004) 218701.
[33] P.S. Dodds, D.J. Watts, A generalized model of social and biological contagion, J. Theoret. Biol. 232 (2005) 587–604.
[34] C.H. Weiss, J. Poncela-Casasnovas, J.I. Glaser, A.R. Pah, S.D. Persell, D.W. Baker, R.G. Wunderink, L.A.N. Amaral, Adoption of a high-impact innovation in a homogeneous population, Phys. Rev. X 4 (2014) 041008.
[35] D. Centola, M. Macy, Complex contagions and the weakness of long ties, Am. J. Sociol. 113 (2007) 702–734.
[36] L. Gao, W. Wang, P. Shu, H. Gao, L.A. Braunstein, Promoting information spreading by using contact memory, Europhys. Lett. 118 (2017) 18001.
[37] D.J. Watts, A simple model of global cascades on random networks, Proc. Natl. Acad. Sci. USA 99 (2002) 5766–5771.
[38] D.E. Whitney, Dynamic theory of cascades on finite clustered random networks with a threshold rule, Phys. Rev. E 82 (2010) 066110.
[39] A. Nematzadeh, E. Ferrara, A. Flammini, Y.-Y. Ahn, Optimal network modularity for information diffusion, Phys. Rev. Lett. 113 (2014) 088701.
[40] K.-M. Lee, C.D. Brummitt, K.-I. Goh, Threshold cascades with response heterogeneity in multiplex networks, Phys. Rev. E 90 (2014) 062816.
[41] C.D. Brummitt, K.-M. Lee, K.-I. Goh, Multiplexity-facilitated cascades in networks, Phys. Rev. E 85 (2012) 045102(R).
[42] O. Yağan, V. Gligor, Analysis of complex contagions in random multiplex networks, Phys. Rev. E 86 (2012) 036103.
[43] P. Shu, L. Gao, P. Zhao, W. Wang, H.E. Stanley, Social contagions on interdependent lattice networks, Sci. Rep. 7 (2017) 44669.
[44] R.R. Liu, W.X. Wang, Y.-C. Lai, B.H. Wang, Cascading dynamics on random networks: Crossover in phase transition, Phys. Rev. E 85 (2012) 026110.
[45] M. Bogũná, C. Castellano, R. Pastor-Satorras, Nature of the epidemic threshold for the susceptible-infected-susceptible dynamics in networks, Phys. Rev. Lett. 111 (2013) 068701.
[46] P. Shu, W. Wang, M. Tang, P. Zhao, Y.-C. Zhang, Recovery rate affects the effective epidemic threshold with synchronous updating, Chaos 26 (2016) 063108.
[47] F. Radicchi, C. Castellano, Breaking of the site-bond percolation universality in networks, Nature Commun. 6 (2015) 10196.
[48] Q.H. Liu, L.F. Zhong, W. Wang, T. Zhou, H.E. Stanley, Chaos 28 (2018) 013120.
[49] L. Speidel, K. Klemm, V.M. Eguíluz, N. Masuda, Temporal interactions facilitate endemicity in the susceptible-infected-susceptible epidemic model, New J. Phys. 18 (2016) 073013.